Molecular structure of tris[(6-bromopyridin-2-yl)methyl]amine

Ran Yan,[a] Zhaohua Dai,[b] Daniel G. Shlian,[a] Trinit'y D. Mitchell,[b] Aaron Loo,[a] Kaltrina Mulosmani[b] and Rita K. Upmacis[b]*

[a]Department of Chemistry, Columbia University, New York, New York 10027, USA, and [b]Department of Chemistry & Physical Sciences, Pace University, New York, New York 10038, USA. *Correspondence e-mail: rupmacis@pace.edu

Coordination compounds of polydentate nitrogen ligands with metals are used extensively in research areas such as catalysis, and as models of complex active sites of enzymes in bioinorganic chemistry. Tris(2-pyridylmethyl)amine (TPA) is a tripodal tetradentate ligand that is known to form coordination compounds with metals, including copper, iron and zinc. The related compound, tris[(6-bromopyridin-2-yl)methyl]amine (TPABr$_3$), $C_{18}H_{15}Br_3N_4$, which possesses a bromine atom on the 6-position of each of the three pyridyl moieties, is also known but has not been heavily investigated. The molecular structure of TPABr$_3$ as determined by X-ray diffraction is reported here. The TPABr$_3$ molecule belongs to the triclinic, $P\bar{1}$ space group and displays interesting intermolecular Br$\cdots$Br interactions that provide a stabilizing influence within the molecule.

1. Chemical context

Tris(2-pyridylmethyl)amine (TPA) was first reported in 1967 (Anderegg & Wenk, 1967), although more recent syntheses are known (Canary *et al.*, 1998; Bazley *et al.*, 2018). TPA is a very versatile ligand and has been used to coordinate metal ions that include, for instance, copper, iron and chromium, thereby forming five- or six-coordinate complexes (Tyeklar *et al.*, 1993; Jang *et al.*, 1991; Gafford & Holwerda, 1990). A more comprehensive review of metal binding to TPA can be found elsewhere (Bravin *et al.*, 2021; Bazley *et al.*, 2018). The TPA ligand has also been successfully employed in the construction of complexes for biological models, for example, copper-cluster enzymes involved in oxygen activation (Maiti *et al.*, 2009) and in iron dioxygenases (Costas *et al.*, 2004). There is also an active interest in pursuing the synthesis of such ligands as biochemical sensors that can rapidly and selectively detect certain metals that are associated with the pathogenesis of diseases, such as Alzheimer's disease (Jomova *et al.*, 2022; Tyczynska *et al.*, 2024). In this regard, TPA has been used to prepare piperidine compounds that can differentially chelate trace metals such as zinc and copper (Dai *et al.*, 2002). In addition to being used in biochemical sensor applications, other areas in which TPA has potential applications include anion sensors, molecular switches, chiral probes and as building blocks in the synthesis of supramolecular cages (Bravin *et al.*, 2021). Despite the prolific use of this ligand, its X-ray structure has only become available within the last ten years and has been chosen as the candidate to introduce crystallography to undergraduate students (Bats & Lerner, 2016; Bazley *et al.*, 2018).

TPA ligands containing various substituted moieties are also known. For instance, TPA containing mono-, bis-, and
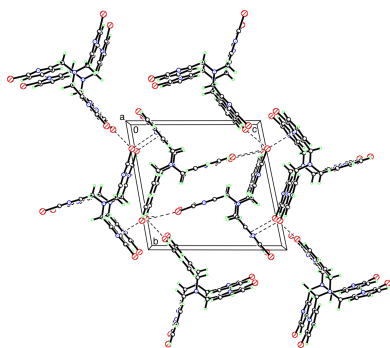
tris-α-methyl substitutions in the ligand complexed to FeCl$_2$ have been characterized (Benhamou *et al.*, 2008). In addition, TPA ligands containing other alkyl or bromo substitutions that are also complexed to iron have been described as well as their ability to catalyze cyclohexane oxygenation by hydrogen peroxide (Guisado-Barrios *et al.*, 2010). Unexpectedly, a high turnover rate and efficient incorporation of oxygen from H$_2$O$_2$ into cyclohexane were reported for the iron complex of TPABr$_3$, which was assumed to have the formula [Fe(TPABr$_3$)(CH$_3$CN)$_2$]$^{2+}$. However, a crystal structure of the TPABr$_3$ ligand with or without the complexed metal has not been reported. Therefore, herein, we describe the molecular structure as determined by X-ray diffraction. The synthesis of TPABr$_3$ is depicted in the scheme and crystals were obtained from a solution in acetonitrile.
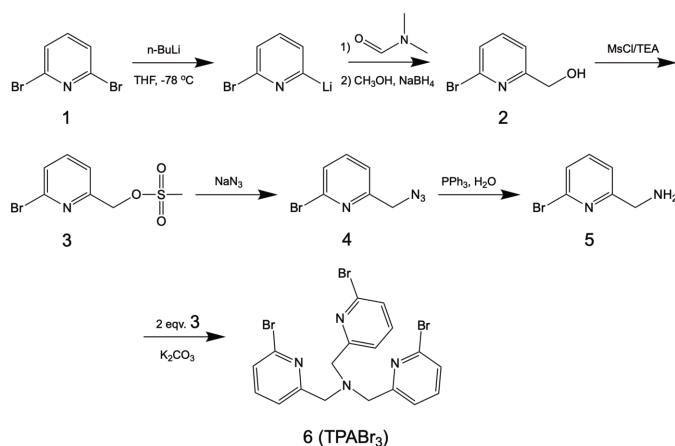
2. Structural commentary

The structure of TPABr$_3$, shown in Fig. 1, reveals that the compound is a tertiary amine with three 6-bromo-2-methyl-pyridine subunits. The central nitrogen atom assumes a trigonal pyramidal geometry with CH$_2$—N4—CH$_2$ angles ranging from 110.4 (4)–111.4 (4)°. The N4—CH$_2$ distances range from 1.456 (6)–1.469 (6) Å for N4—C1, N4—C2, and N4—C3. The C—Br distances range from 1.905 (6)–1.920 (6) Å for the C15—Br1, C25—Br2 and C35—Br3 bond

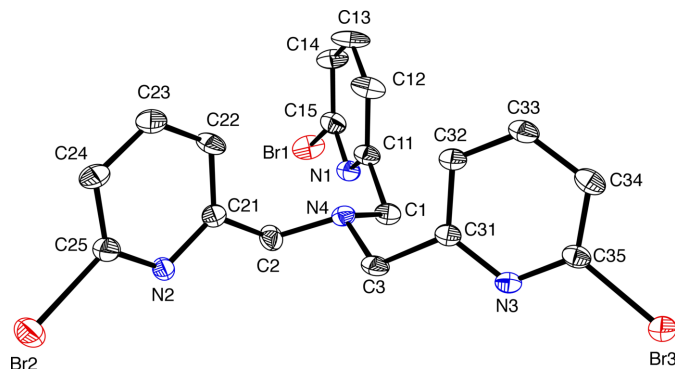lengths, which compare well with the C—Br distances in the tris(bromopyrazolylmethyl)amine ligand that measure 1.881 (5) Å (Haldón *et al.*, 2014).

3. Supramolecular features

Fig. 2 shows the packing in the unit cell along the *a*-axis direction. There are no significant intermolecular hydrogen-bonding interactions. However, there are intramolecular distances of 2.852, 2.765 and 2.793 Å for N4···H12*A*, N4···H22*A* and N4···H32*A*, respectively, which at best, may indicate a very weak interaction.

The unit cell also shows two intermolecular Br···Br interactions, with Br2···Br3 at 3.6540 (11) Å and Br1···Br3 at 3.7731 (11) Å, which are close to the sum of the van der Waals radii, which is approximately 3.7 Å for Br···Br. Interestingly, C—Br···Br—C interactions can occur over a 3.0–4.5 Å range and provide a stabilizing influence within the crystal (Capdevila-Cortada & Novoa, 2015). The strength of the halogen–halogen interaction depends on the halogen atom in the following order: I > Br > Cl > F (Awwadi *et al.*, 2006). It has previously been noted that R—Br···Br—R contacts can occur according to two different geometries, classified as type I (symmetrical interactions where $\theta_1 = \theta_2$) and type II (bent interactions where $\theta_1 \simeq 180°$ and $\theta_2 \simeq 90°$) (Sakurai *et al.*, 1963; Desiraju & Parthasarathy, 1989; Cavallo *et al.*, 2016). In TPABr$_3$, θ_1 and θ_2 are 160.82 and 74.14° for C15—Br1···Br3—C35, and 176.97 and 87.15° for C25—Br2···Br3—C35, respectively, indicating that they are type II interactions.

For comparison, the packing in the unit cell of the related tris(bromopyrazolylmethyl)amine ligand is arranged in a different fashion, displaying intermolecular pyrazolyl N···Br distances of 3.099 Å (Haldón *et al.*, 2014). The N—C—N—N torsion angle (from the central nitrogen atom to the nitrogen

Figure 1
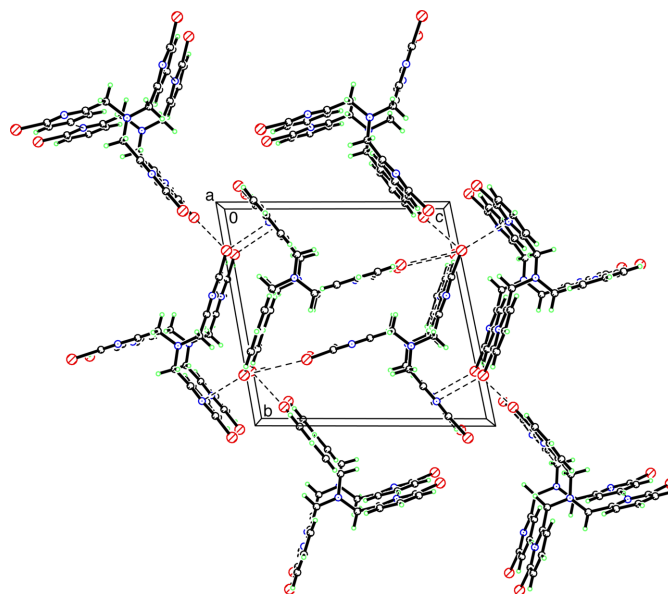Crystal structure of TPABr$_3$. Displacement ellipsoids are drawn at the 30% probability level.

Figure 2
Unit-cell packing of TPABr$_3$.

atoms in the pyrazolyl ring) is between 95.20 and 95.25° compared to the corresponding values of 122.2 (5)–132.6 (5)° in TPABr$_3$ for the N—C—C—N bonds, indicating the different degrees of rotation of the pyrazolyl *versus* pyridyl rings.

4. Database survey

Much effort has been expended synthesizing TPA ligands that contain novel substitutions on the pyridyl rings. For instance, TPA derivatives containing the following types of groups have been reported: (i) tripodal tetradentate ligands containing pyridyl-pivalamido groups have been prepared and complexed to copper and zinc ions (Harata *et al.*, 1998; Rivas *et al.*, 2003); (ii) TPA ligands containing pyridyl-trimethoxy-phenyl groups have been synthesized (and complexed with copper and zinc ions) in an effort to enhance their solubility in aqueous and common organic solvents (Liang *et al.*, 2009); (iii) TPA-related derivatives containing carboxylic acid functionalities on the pyridyl rings have been synthesized and their complexation to gadolinium investigated (Bretonnière *et al.*, 2001); (iv) a TPA derivative containing thiourea substitutions has been prepared and coordinated with different transition metal ions, forming seven co-ordinate Mn^{II} and Cd^{II}, six co-ordinate Ni^{II} and five co-ordinate Co^{II}, Cu^{II} and Zn^{II} complexes (Saad *et al.*, 2012); (v) sulfonyl subunits have been attached to the pyridyl rings in order to make TPA highly water compatible, which allows for broader applicability to the biomedical arena (Salaam *et al.*, 2020); (vi) isoquinoline-derivatized TPAs have been prepared for use as fluorescent zinc sensors (Mikata *et al.*, 2014, 2015), and (vii) other TPA-based ligands that have been prepared include those possessing phenylethynyl units and their copper(II) complexes investigated (Lim *et al.*, 2016). Furthermore, TPA ligands containing one and two chiral substituents on the tripodal skeleton have been synthesized using lipase enzyme and lanthanide complexation investigated (Yamada *et al.*, 2003).

Tripod ligands containing pyrazolyl rather than pyridyl rings are also known. In this regard, novel tris-(pyrazolylmethyl)amine ligands that contain methyl and bromo substituents on the pyrazolyl moiety have been synthesized and structurally characterized (Haldón *et al.*, 2014). The catalytic activities of the copper(I) complexes of these ligands were explored in carbene- and nitrene-transfer studies. In this case, the crystal structure for the tris(bromo-pyrazolylmethyl)amine ligand is known (Haldón *et al.*, 2014).

5. Synthesis and crystallization

The synthesis of TPABr$_3$ is shown in the Scheme. The starting material, 2,6-dibromopyridine (Compound **1**), was reacted with *n*-butyllithium at 195 K to generate 2-bromo-6-lithio-pyridine (not isolated), which was subsequently reacted with DMF followed by reduction with NaBH$_4$ to give (6-bromo-2-pyridyl)methanol (compound **2**). Using methanesulfonyl chloride (MsCl) and triethylamine (TEA), the alcohol compound **2** was converted to a mesylate compound **3**.

Table 1
Experimental details.

Crystal data	
Chemical formula	C$_{18}$H$_{15}$Br$_3$N$_4$
M_r	527.07
Crystal system, space group	Triclinic, $P\bar{1}$
Temperature (K)	180
a, b, c (Å)	6.2445 (8), 13.2335 (16), 13.4984 (16)
α, β, γ (°)	79.168 (2), 88.671 (2), 78.962 (2)
V (Å^3)	1075.2 (2)
Z	2
Radiation type	Mo $K\alpha$
μ (mm^{-1})	5.64
Crystal size (mm)	0.15 × 0.13 × 0.04
Data collection	
Diffractometer	Bruker APEXII CCD
Absorption correction	Multi-scan (*SADABS*; Krause *et al.*, 2015)
T_{min}, T_{max}	0.535, 0.746
No. of measured, independent and observed [$I > 2\sigma(I)$] reflections	11638, 3813, 2434
R_{int}	0.070
$(\sin \theta/\lambda)_{max}$ (Å^{-1})	0.595
Refinement	
$R[F^2 > 2\sigma(F^2)]$, $wR(F^2)$, S	0.045, 0.114, 1.02
No. of reflections	3813
No. of parameters	226
H-atom treatment	H-atom parameters constrained
$\Delta\rho_{max}, \Delta\rho_{min}$ (e Å^{-3})	0.47, −0.67

Computer programs: *APEX4* and *SAINT* (Bruker, 2014), *SHELXT* (Sheldrick 2015a), *SHELXL2019/1* (Sheldrick, 2015b) and *SHELXTL* (Sheldrick, 2008).

Mesylate **3** was reacted with NaN$_3$ in an S$_N$2 reaction to afford the organic azide (compound **4**), which was subsequently reduced by PPh$_3$ to a primary amine (compound **5**). Reacting compound **5** with two equivalents of mesylate compound **3** resulted in the target compound TPABr$_3$ **6**, with an overall yield of 49%.

The resulting compound, TPABr$_3$ (0.0133 g; 0.024 mmol), was dissolved in acetonitrile (CH$_3$CN; 2 mL) and allowed to evaporate. After 4 days at ambient temperature, colorless needles of TPABr$_3$, suitable for X-ray diffraction, were crystallized from the solution.

6. Refinement

Crystal data, data collection and structure refinement details are summarized in Table 1. Hydrogen atoms on carbon were placed in calculated positions and included as riding contributions with isotropic displacement parameters U_{iso}(H) = 1.2U_{eq}(Csp^2) or 1.5U_{eq}(Csp^3) using *SHELXL2019/1* (Sheldrick, 2015b). The structure contained poorly defined acetonitrile solvent molecules that were removed by the SQUEEZE procedure in *PLATON* (Spek, 2015), which identified a void volume of 167 Å^3 containing approximately 47 electrons.

Acknowledgements

References

Anderegg, G. & Wenk, F. (1967). *Helv. Chim. Acta*, **50**, 2330–2332.

Awwadi, F. F., Willett, R. D., Peterson, K. A. & Twamley, B. (2006). *Chem. A Eur. J.* **12**, 8952–8960.

Bats, W. J. & Lerner, H.-W. (2016). *Crystal Structure Determination* (CCDC 1005049). CCDC, Ca, bridge, England. https://doi.org/10.5517/ccdc. csd. cc12qtyk.

Bazley, I. J., Erie, E. A., Feiereisel, G. M., LeWarne, C. J., Peterson, J. M., Sandquist, K. L., Oshin, K. D. & Zeller, M. (2018). *J. Chem. Educ.* **95**, 876–881.

Benhamou, L., Lachkar, M., Mandon, D. & Welter, R. (2008). *Dalton Trans.* pp. 6996–7003.

Bravin, C., Badetti, E., Licini, G. & Zonta, C. (2021). *Coord. Chem. Rev.* **427**, 213558.

Bretonnière, Y., Mazzanti, M., Pécaut, J., Dunand, F. A. & Merbach, A. E. (2001). *Inorg. Chem.* **40**, 6737–6745.

Bruker (2014). *APEX4* and *SAINT*. Bruker AXS Inc., Madison, Wisconsin, USA.

Canary, J. W., Wang, Y. H., Roy, R., Que, L. & Miyake, H. (1998). *Inorg. Synth.* **32**, 70–75.

Capdevila-Cortada, M. & Novoa, J. J. (2015). *CrystEngComm*, **17**, 3354–3365.

Cavallo, G., Metrangolo, P., Milani, R., Pilati, T., Priimagi, A., Resnati, G. & Terraneo, G. (2016). *Chem. Rev.* **116**, 2478–2601.

Costas, M., Mehn, M. P., Jensen, M. P. & Que, L. (2004). *Chem. Rev.* **104**, 939–986.

Dai, Z. H., Xu, X. D. & Canary, J. W. (2002). *Chem. Commun.* pp. 1414–1415.

Desiraju, G. R. & Parthasarathy, R. (1989). *J. Am. Chem. Soc.* **111**, 8725–8726.

Gafford, B. G. & Holwerda, R. A. (1990). *Inorg. Chem.* **29**, 233–238.

Guisado-Barrios, G., Slawin, A. M. Z. & Richens, D. T. (2010). *J. Coord. Chem.* **63**, 2642–2658.

Haldón, E., Delgado-Rebollo, M., Prieto, A., Álvarez, E., Maya, C., Nicasio, M. C. & Pérez, P. J. (2014). *Inorg. Chem.* **53**, 4192–4201.

Harata, M., Hasegawa, K., Jitsukawa, K., Masuda, H. & Einaga, H. (1998). *Bull. Chem. Soc. Jpn*, **71**, 1031–1038.

Jang, H. G., Cox, D. D. & Que, L. (1991). *J. Am. Chem. Soc.* **113**, 9200–9204.

Jomova, K., Makova, M., Alomar, S. Y., Alwasel, S. H., Nepovimova, E., Kuca, K., Rhodes, C. J. & Valko, M. (2022). *Chem. Biol. Interact.* **367**, 110173.

Krause, L., Herbst-Irmer, R., Sheldrick, G. M. & Stalke, D. (2015). *J. Appl. Cryst.* **48**, 3–10.

Liang, J., Zhang, J., Zhu, L., Duarandin, A., Young, V. G., Geacintov, N. & Canary, J. W. (2009). *Inorg. Chem.* **48**, 11196–11208.

Lim, J., Lynch, V. M., Edupuganti, R., Ellington, A. & Anslyn, E. V. (2016). *Dalton Trans.* **45**, 10585–10598.

Maiti, D., Woertink, J. S., Ghiladi, R. A., Solomon, E. I. & Karlin, K. D. (2009). *Inorg. Chem.* **48**, 8342–8356.

Mareque Rivas, J. C., Torres Martín de Rosales, R. & Parsons, S. (2003). *Dalton Trans.* pp. 2156–2163.

Mikata, Y., Kawata, K., Takeuchi, S., Nakanishi, K., Konno, H., Itami, S., Yasuda, K., Tamotsu, S. & Burdette, S. C. (2014). *Dalton Trans.* **43**, 10751–10759.

Mikata, Y., Nodomi, Y., Ohnishi, R., Kizu, A. & Konno, H. (2015). *Dalton Trans.* **44**, 8021–8030.

Saad, F. A., Buurma, N. J., Amoroso, A. J., Knight, J. C. & Kariuki, B. M. (2012). *Dalton Trans.* **41**, 4608–4617.

Sakurai, T., Sundaralingam, M. & Jeffrey, G. A. (1963). *Acta Cryst.* **16**, 354–363.

Salaam, J., Pilet, G. & Hasserodt, J. (2020). *Inorg. Chem.* **59**, 13812–13816.

Sheldrick, G. M. (2008). *Acta Cryst.* A**64**, 112–122.

Sheldrick, G. M. (2015a). *Acta Cryst.* A**71**, 3–8.

Sheldrick, G. M. (2015b). *Acta Cryst.* C**71**, 3–8.

Spek, A. L. (2015). *Acta Cryst.* C**71**, 9–18.

Tyczyńska, M., Gędek, M., Brachet, A., Stręk, W., Flieger, J., Teresiński, G. & Baj, J. (2024). *J. Clin. Med.* **13**, 2381.

Tyeklar, Z., Jacobson, R. R., Wei, N., Murthy, N. N., Zubieta, J. & Karlin, K. D. (1993). *J. Am. Chem. Soc.* **115**, 2677–2689.

Yamada, T., Shinoda, S., Sugimoto, H., Uenishi, J. & Tsukube, H. (2003). *Inorg. Chem.* **42**, 7932–7937.

Molecular structure of tris[(6-bromopyridin-2-yl)methyl]amine

Ran Yan, Zhaohua Dai, Daniel G. Shlian, Trinit'y D. Mitchell, Aaron Loo, Kaltrina Mulosmani and Rita K. Upmacis

Computing details

Tris[(6-bromopyridin-2-yl)methyl]amine

Crystal data

$C_{18}H_{15}Br_3N_4$	$Z = 2$
$M_r = 527.07$	$F(000) = 512$
Triclinic, $P\overline{1}$	$D_x = 1.628$ Mg m^{-3}
$a = 6.2445$ (8) Å	Mo $K\alpha$ radiation, $\lambda = 0.71073$ Å
$b = 13.2335$ (16) Å	Cell parameters from 3031 reflections
$c = 13.4984$ (16) Å	$\theta = 3.1–23.8°$
$\alpha = 79.168$ (2)°	$\mu = 5.64$ mm^{-1}
$\beta = 88.671$ (2)°	$T = 180$ K
$\gamma = 78.962$ (2)°	Plate, colorless
$V = 1075.2$ (2) Å^3	$0.15 \times 0.13 \times 0.04$ mm

Data collection

Bruker APEXII CCD diffractometer	3813 independent reflections
φ and ω scans	2434 reflections with $I > 2\sigma(I)$
Absorption correction: multi-scan (SADABS; Krause *et al.*, 2015)	$R_{int} = 0.070$
	$\theta_{max} = 25.0°$, $\theta_{min} = 1.5°$
$T_{min} = 0.535$, $T_{max} = 0.746$	$h = -7\rightarrow7$
11638 measured reflections	$k = -15\rightarrow15$
	$l = -16\rightarrow16$

Refinement

Refinement on F^2	Hydrogen site location: inferred from neighbouring sites
Least-squares matrix: full	
$R[F^2 > 2\sigma(F^2)] = 0.045$	H-atom parameters constrained
$wR(F^2) = 0.114$	$w = 1/[\sigma^2(F_o^2) + (0.0464P)^2]$
$S = 1.02$	where $P = (F_o^2 + 2F_c^2)/3$
3813 reflections	$(\Delta/\sigma)_{max} < 0.001$
226 parameters	$\Delta\rho_{max} = 0.47$ e Å^{-3}
0 restraints	$\Delta\rho_{min} = -0.67$ e Å^{-3}
Primary atom site location: dual	

Special details

Geometry. All esds (except the esd in the dihedral angle between two l.s. planes) are estimated using the full covariance matrix. The cell esds are taken into account individually in the estimation of esds in distances, angles and torsion angles; correlations between esds in cell parameters are only used when they are defined by crystal symmetry. An approximate (isotropic) treatment of cell esds is used for estimating esds involving l.s. planes.

Fractional atomic coordinates and isotropic or equivalent isotropic displacement parameters (Å²)

	x	*y*	*z*	U_{iso}*/U_{eq}
N1	0.2019 (7)	0.3566 (4)	0.5337 (3)	0.0361 (12)
N2	0.2962 (7)	0.0992 (3)	0.2191 (3)	0.0326 (11)
N3	0.1478 (7)	0.5757 (4)	0.0911 (3)	0.0297 (11)
N4	0.2814 (7)	0.3485 (3)	0.2805 (3)	0.0289 (11)
C1	0.1888 (9)	0.4160 (5)	0.3517 (4)	0.0339 (14)
H1B	0.033813	0.410977	0.363630	0.041*
H1C	0.195167	0.489831	0.322584	0.041*
C2	0.2338 (9)	0.2435 (4)	0.3100 (4)	0.0375 (14)
H2B	0.082095	0.244305	0.289608	0.045*
H2C	0.245189	0.222326	0.384317	0.045*
C3	0.2015 (8)	0.3948 (4)	0.1774 (4)	0.0352 (14)
H3B	0.040155	0.413243	0.177665	0.042*
H3C	0.242935	0.342154	0.133650	0.042*
C11	0.3149 (9)	0.3831 (5)	0.4508 (4)	0.0362 (14)
C12	0.5393 (10)	0.3798 (5)	0.4535 (5)	0.0520 (18)
H12A	0.615838	0.397766	0.393057	0.062*
C13	0.6481 (10)	0.3503 (6)	0.5449 (5)	0.062 (2)
H13A	0.800619	0.348382	0.548534	0.074*
C14	0.5330 (9)	0.3234 (5)	0.6310 (5)	0.0505 (18)
H14A	0.602337	0.302168	0.695444	0.061*
C15	0.3143 (10)	0.3290 (5)	0.6190 (4)	0.0426 (15)
C21	0.3881 (8)	0.1643 (4)	0.2622 (4)	0.0309 (13)
C22	0.6111 (9)	0.1585 (5)	0.2635 (4)	0.0398 (15)
H22A	0.671672	0.206481	0.293351	0.048*
C23	0.7461 (9)	0.0826 (5)	0.2212 (4)	0.0446 (16)
H23A	0.899873	0.077695	0.221881	0.054*
C24	0.6541 (9)	0.0143 (5)	0.1780 (5)	0.0444 (16)
H24A	0.740674	−0.039675	0.149128	0.053*
C25	0.4311 (9)	0.0285 (5)	0.1790 (5)	0.0407 (15)
C31	0.2914 (8)	0.4916 (4)	0.1340 (4)	0.0275 (13)
C32	0.5142 (8)	0.4917 (5)	0.1382 (4)	0.0339 (14)
H32A	0.612525	0.430920	0.170020	0.041*
C33	0.5894 (9)	0.5802 (4)	0.0960 (4)	0.0355 (14)
H33A	0.740996	0.581301	0.097381	0.043*
C34	0.4421 (9)	0.6686 (5)	0.0512 (4)	0.0367 (15)
H34A	0.488557	0.731787	0.021853	0.044*
C35	0.2253 (8)	0.6605 (5)	0.0512 (4)	0.0322 (14)
Br1	0.14783 (11)	0.28852 (6)	0.73619 (5)	0.0588 (2)
Br2	0.29223 (11)	−0.06206 (6)	0.11734 (6)	0.0598 (2)
Br3	0.01178 (10)	0.77792 (5)	−0.00858 (5)	0.0454 (2)

Atomic displacement parameters (Å²)

	U^{11}	U^{22}	U^{33}	U^{12}	U^{13}	U^{23}
N1	0.031 (3)	0.042 (3)	0.038 (3)	−0.008 (2)	0.001 (2)	−0.013 (2)

N2	0.024 (2)	0.029 (3)	0.048 (3)	−0.006 (2)	0.002 (2)	−0.013 (2)
N3	0.027 (3)	0.037 (3)	0.026 (2)	−0.008 (2)	−0.003 (2)	−0.007 (2)
N4	0.026 (2)	0.034 (3)	0.027 (3)	−0.003 (2)	−0.0025 (19)	−0.009 (2)
C1	0.032 (3)	0.046 (4)	0.026 (3)	−0.010 (3)	0.000 (2)	−0.008 (3)
C2	0.035 (3)	0.034 (4)	0.046 (4)	−0.012 (3)	0.008 (3)	−0.007 (3)
C3	0.021 (3)	0.046 (4)	0.042 (4)	−0.011 (3)	0.000 (2)	−0.012 (3)
C11	0.027 (3)	0.047 (4)	0.039 (4)	−0.010 (3)	0.004 (3)	−0.020 (3)
C12	0.037 (4)	0.081 (5)	0.047 (4)	−0.026 (4)	0.004 (3)	−0.020 (4)
C13	0.022 (3)	0.109 (6)	0.062 (5)	−0.024 (4)	−0.002 (3)	−0.022 (4)
C14	0.032 (4)	0.078 (5)	0.044 (4)	−0.007 (3)	−0.008 (3)	−0.017 (4)
C15	0.039 (4)	0.051 (4)	0.042 (4)	−0.014 (3)	0.002 (3)	−0.017 (3)
C21	0.029 (3)	0.033 (3)	0.030 (3)	−0.004 (3)	0.001 (2)	−0.005 (3)
C22	0.029 (3)	0.050 (4)	0.048 (4)	−0.021 (3)	0.002 (3)	−0.012 (3)
C23	0.023 (3)	0.050 (4)	0.061 (4)	−0.008 (3)	0.004 (3)	−0.010 (4)
C24	0.020 (3)	0.049 (4)	0.064 (4)	−0.001 (3)	0.003 (3)	−0.017 (3)
C25	0.033 (3)	0.037 (4)	0.052 (4)	−0.010 (3)	−0.007 (3)	−0.003 (3)
C31	0.028 (3)	0.037 (4)	0.019 (3)	−0.009 (3)	0.001 (2)	−0.009 (3)
C32	0.022 (3)	0.042 (4)	0.038 (3)	−0.007 (3)	0.000 (2)	−0.008 (3)
C33	0.024 (3)	0.044 (4)	0.044 (4)	−0.011 (3)	0.003 (3)	−0.017 (3)
C34	0.033 (3)	0.047 (4)	0.037 (3)	−0.018 (3)	0.009 (3)	−0.017 (3)
C35	0.029 (3)	0.040 (4)	0.033 (3)	−0.010 (3)	0.001 (2)	−0.016 (3)
Br1	0.0457 (4)	0.0890 (6)	0.0383 (4)	−0.0084 (4)	0.0041 (3)	−0.0086 (4)
Br2	0.0428 (4)	0.0583 (5)	0.0889 (6)	−0.0087 (3)	−0.0046 (4)	−0.0410 (4)
Br3	0.0343 (4)	0.0423 (4)	0.0574 (4)	−0.0095 (3)	−0.0085 (3)	−0.0009 (3)

Geometric parameters (Å, º)

N1—C15	1.317 (7)	C13—C14	1.378 (8)
N1—C11	1.335 (7)	C14—C15	1.366 (8)
N2—C25	1.320 (7)	C15—Br1	1.920 (6)
N2—C21	1.343 (6)	C21—C22	1.381 (7)
N3—C35	1.324 (6)	C22—C23	1.384 (8)
N3—C31	1.334 (6)	C23—C24	1.378 (8)
N4—C2	1.456 (6)	C24—C25	1.369 (7)
N4—C1	1.468 (6)	C25—Br2	1.920 (6)
N4—C3	1.469 (6)	C31—C32	1.394 (7)
C1—C11	1.516 (7)	C32—C33	1.365 (7)
C2—C21	1.511 (7)	C33—C34	1.389 (8)
C3—C31	1.509 (7)	C34—C35	1.378 (7)
C11—C12	1.395 (8)	C35—Br3	1.905 (6)
C12—C13	1.376 (8)		
C15—N1—C11	116.0 (5)	N2—C21—C22	121.9 (5)
C25—N2—C21	116.3 (5)	N2—C21—C2	116.2 (5)
C35—N3—C31	117.2 (4)	C22—C21—C2	121.9 (5)
C2—N4—C1	111.4 (4)	C21—C22—C23	119.7 (5)
C2—N4—C3	110.4 (4)	C24—C23—C22	119.0 (5)
C1—N4—C3	110.9 (4)	C25—C24—C23	116.4 (6)

N4—C1—C11	110.2 (4)	N2—C25—C24	126.7 (5)
N4—C2—C21	111.9 (4)	N2—C25—Br2	114.8 (4)
N4—C3—C31	112.6 (4)	C24—C25—Br2	118.5 (5)
N1—C11—C12	122.4 (5)	N3—C31—C32	122.2 (5)
N1—C11—C1	117.0 (5)	N3—C31—C3	116.7 (4)
C12—C11—C1	120.6 (5)	C32—C31—C3	121.1 (5)
C13—C12—C11	119.0 (6)	C33—C32—C31	119.3 (5)
C12—C13—C14	119.1 (6)	C32—C33—C34	119.3 (5)
C15—C14—C13	116.6 (6)	C35—C34—C33	116.9 (5)
N1—C15—C14	126.8 (6)	N3—C35—C34	125.1 (5)
N1—C15—Br1	114.9 (4)	N3—C35—Br3	115.1 (4)
C14—C15—Br1	118.3 (5)	C34—C35—Br3	119.8 (4)
C2—N4—C1—C11	71.5 (5)	N4—C2—C21—C22	47.9 (7)
C3—N4—C1—C11	−165.2 (4)	N2—C21—C22—C23	−1.3 (9)
C1—N4—C2—C21	−159.9 (4)	C2—C21—C22—C23	178.2 (5)
C3—N4—C2—C21	76.5 (5)	C21—C22—C23—C24	0.3 (9)
C2—N4—C3—C31	−166.5 (4)	C22—C23—C24—C25	1.1 (9)
C1—N4—C3—C31	69.6 (5)	C21—N2—C25—C24	0.7 (9)
C15—N1—C11—C12	1.3 (9)	C21—N2—C25—Br2	−179.5 (4)
C15—N1—C11—C1	−179.6 (5)	C23—C24—C25—N2	−1.7 (10)
N4—C1—C11—N1	−122.2 (5)	C23—C24—C25—Br2	178.6 (5)
N4—C1—C11—C12	57.0 (7)	C35—N3—C31—C32	0.6 (7)
N1—C11—C12—C13	−1.3 (10)	C35—N3—C31—C3	−178.9 (4)
C1—C11—C12—C13	179.6 (6)	N4—C3—C31—N3	−131.2 (5)
C11—C12—C13—C14	0.8 (11)	N4—C3—C31—C32	49.3 (7)
C12—C13—C14—C15	−0.4 (10)	N3—C31—C32—C33	−0.9 (8)
C11—N1—C15—C14	−0.9 (9)	C3—C31—C32—C33	178.6 (5)
C11—N1—C15—Br1	−178.7 (4)	C31—C32—C33—C34	0.9 (8)
C13—C14—C15—N1	0.5 (10)	C32—C33—C34—C35	−0.7 (8)
C13—C14—C15—Br1	178.2 (5)	C31—N3—C35—C34	−0.4 (8)
C25—N2—C21—C22	0.8 (8)	C31—N3—C35—Br3	−179.9 (4)
C25—N2—C21—C2	−178.7 (5)	C33—C34—C35—N3	0.5 (8)
N4—C2—C21—N2	−132.6 (5)	C33—C34—C35—Br3	180.0 (4)